Electronic Supplementary Information

Modulation of properties with dinulear lanthanide complexes through utilizing different *β*-diketone co-ligands: near-infrared luminescence and magnetization dynamics

Yun-Juan Wang,[a] Dong-Fang Wu,[a] Jian Gou,[a] Yao-Yao Duan,[a] Ling Li,[a] Huan-Huan Chen,[a] Hong-Ling Gao*[a,b] and Jian-Zhong Cui*[a,b]

List of contents

Section S1 Supplementary Experimental Section

Section S2 Powder X-ray Diffraction, UV-Vis specta, Photoluminescence properties and Near-infrared luminescence spectra

Section S3 Plots of Magnetic Data

Section S4 Crystallographic Data and Continuous Shape Measures Values

[a]*Department of Chemistry, Tianjin University, Tianjin, 300354, China.*
* *Corresponding authors, E-mail: cuijianzhong@tju.edu.cn, ghl@tju.edu.cn.*
[b]*Key Laboratory of Advanced Energy Materials Chemistry (Ministry of Education), Nankai University, Tianjin, 300071, China.*

Scheme S1 The synthesis of N'-(2-hydroxy-5-methylphenyl)-pyrazine-2-carbohydrazide (H_2L).

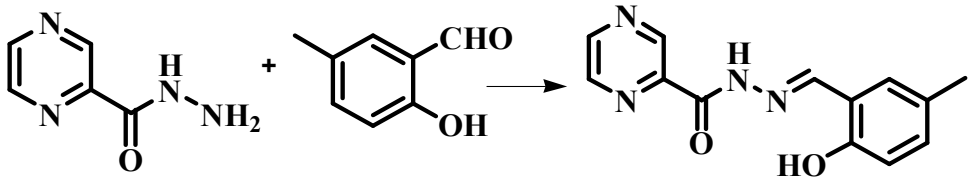

To a solution of 2-hydroxy-5-methylbenzaldehyde (10 mmol) in ethanol was added a solution of pyrazine-2-carbohydrazide (10 mmol) [1] in ethanol (Scheme S1). The reaction mixture is stirred overnight at room temperature, a crude product was obtained, which was washed with ethanol and dried in vacuo to give the H_2L ligand as a light apricot solid. The pale apricot precipitate was heated to reflux in methanol and recrystallized to give a light yellow needle-like crystalline solid. Yield: *ca*. 80%. Elemental analysis (%), calcd for $C_{13}H_{12}N_4O_3$ (fw = 256.27): C, 60.87; H, 4.68; N, 21.85. Found: C, 61.27; H, 4.98; N, 21.44. ^{1}H NMR (d_6-DMSO, δ/ppm): 2.26(3H, C–H), 3.17(1H, C–H), 6.84, 7.13, 7.33(3H, C–H), 8.80, 8.97, 9.30(3H, C–H), 11.07(1H, N–H), 12.68 (1H, O–H) (^{1}H NMR spectrum of H_2L is shown in Fig. S1, ESI†)

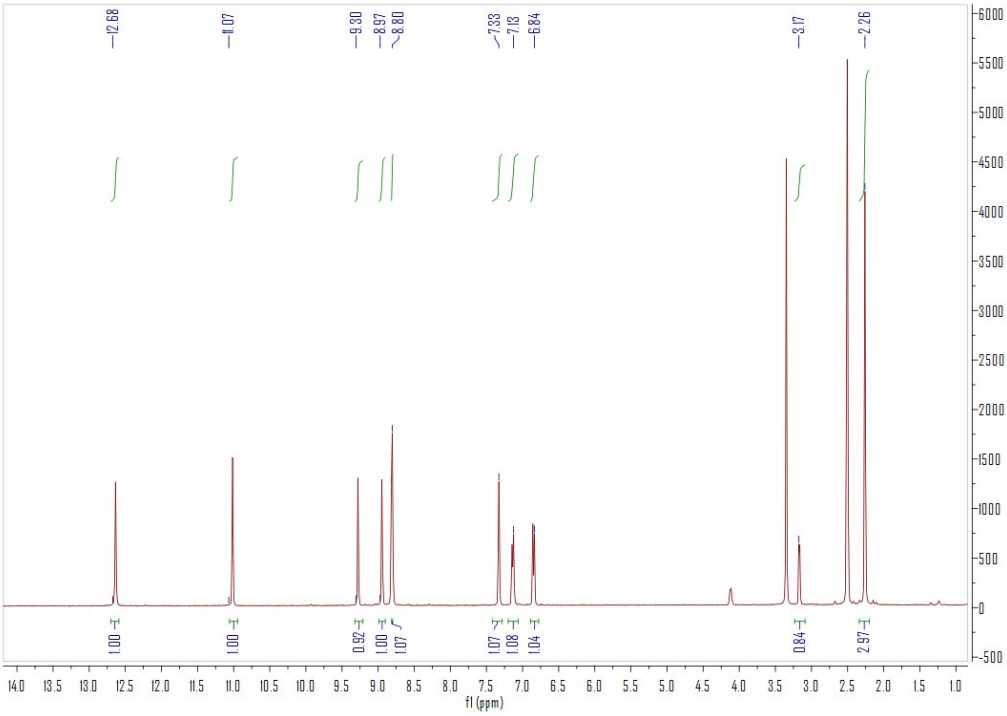

Fig. S1 ^{1}H NMR spectrum (400 MHz, d_6-DMSO) of H_2L.

Scheme S2 Powder X-ray diffraction (PXRD)

The phase purity of crystalline samples of **1**−**10** were characterized by powder X-ray diffraction (PXRD) at room temperature (Fig. S2, ESI†). The experimental peaks conform with those simulated from the single crystal X-ray diffraction data.

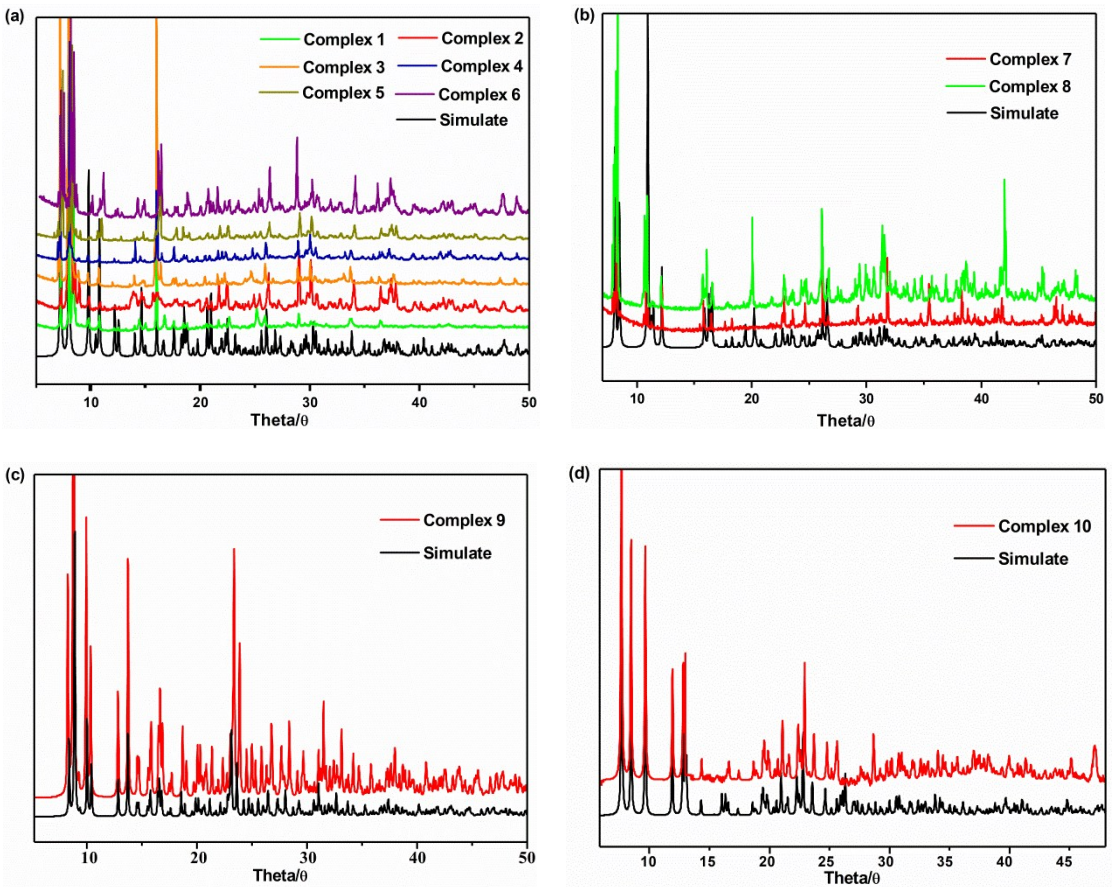

Fig. S2 PXRD patterns of complexes **1-6**(a), **7-8**(b), **9**(c) and **10**(d).

UV-Vis spectra

The UV-Vis absorption spectra of $Dy(dbm)_3{\cdot}2H_2O$, $Dy(acac)_3{\cdot}2H_2O$, $Dy(TTA)_3{\cdot}2H_2O$, $Dy(tfa)_3{\cdot}2H_2O$, the ligand H_2L and complexes **1**−**10** in dichloromethane solutions were measured in the range of 200–600 nm at room temperature (Fig. S3, ESI†). For the ligand H_2L, three main absorption bands were observed at *ca*. 238, 293, and 351 nm, respectively. As fig. S3 (a) shows, for $Dy(dbm)_3$, it shows two absorption bands at *ca*. 237 and 345 nm; and **1**−**6** show similar absorption curves at *ca*. 238, 337 and 416 nm due to the n → π* and π → π* transitions of ligands L^{2-} and dbm^-. Obviously, the bands appears to be red-shifted as a whole, which is the result of the introduction of dbm^- with an increase in the degree of conjugation. The $Dy(acac)_3{\cdot}2H_2O$ has two absorption bands centered at *ca*. 224 and 287 nm in the fig. S3 (b), and for **7**−**8** there are four absorption bands centered at *ca*. 239, 270, 298 and 397 nm (n → π* and π → π* transitions of ligands L^{2-} and $acac^-$). Fig. S3 (c) displays that the absorption bands of $Dy(TTA)_3{\cdot}2H_2O$ are found at *ca*. 237, 275, and 341 nm and three absorption bands situated at *ca*.234, 271 and 340 nm for **9** (n → π* and π → π* transitions of ligands L^{2-} and TTA^-). Analogously, two primary absorption bands centered at *ca*. 233 and 292 nm can be observed for $Dy(tfa)_3{\cdot}2H_2O$, and **10** possesses three absorption bands centered at *ca*. 237, 300 and 396 nm (n → π* and π → π* transitions of ligands L^{2-} and tfa^-). In short, the absorption band positions of **1**−**10** are slightly different compared to the ligand H_2L own to the influence of different *β*-diketone co-ligands.

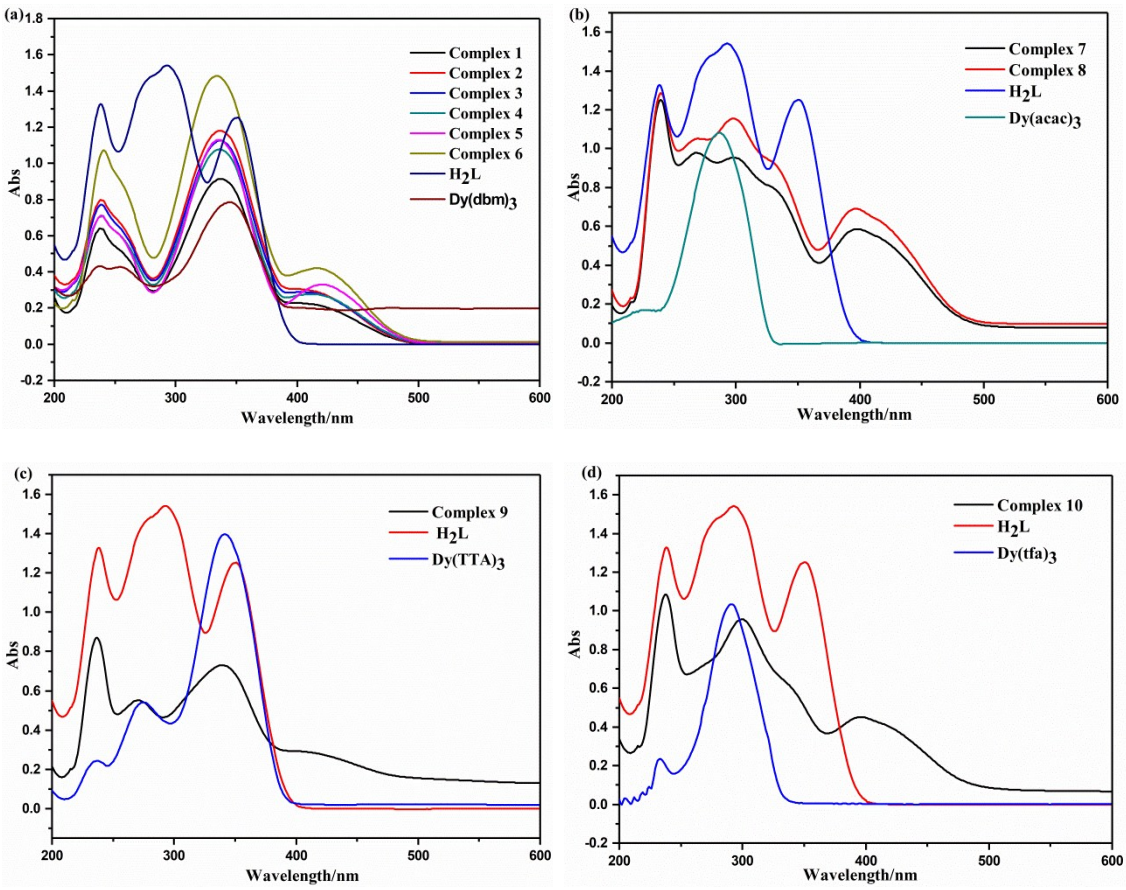

Fig. S3 The UV-vis absorption spectra of $Dy(dbm)_3 \cdot 2H_2O$, $Dy(acac)_3 \cdot 2H_2O$, $Dy(TTA)_3 \cdot 2H_2O$, $Dy(tfa)_3 \cdot 2H_2O$, the ligand H_2L and complexes **1–10**.

Photoluminescence properties

The photoluminescence of complex **1** was measured in dichloromethane solution at room temperature. The emission spectrum of **1** at excitation wavelength of 335 nm reveals four characteristic emission bands of Tb^{3+}, corresponding to the $^5D_4 \rightarrow {}^7F_6$ (495nm), $^5D_4 \rightarrow {}^7F_5$ (536nm), $^5D_4 \rightarrow {}^7F_4$ (580nm), $^5D_4 \rightarrow {}^7F_3$ (605nm), respectively. Among them, the $^5D_4 \rightarrow {}^7F_5$ transition is the strongest (Fig. S4, ESI†).

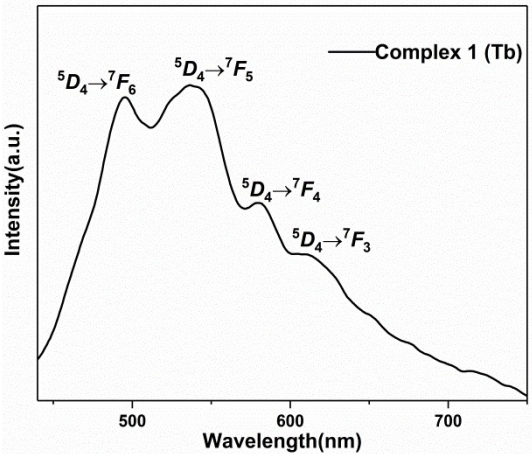

Fig. S4 Room-temperature photoluminescence spectrum of complex **1** in dichloromethane solution.

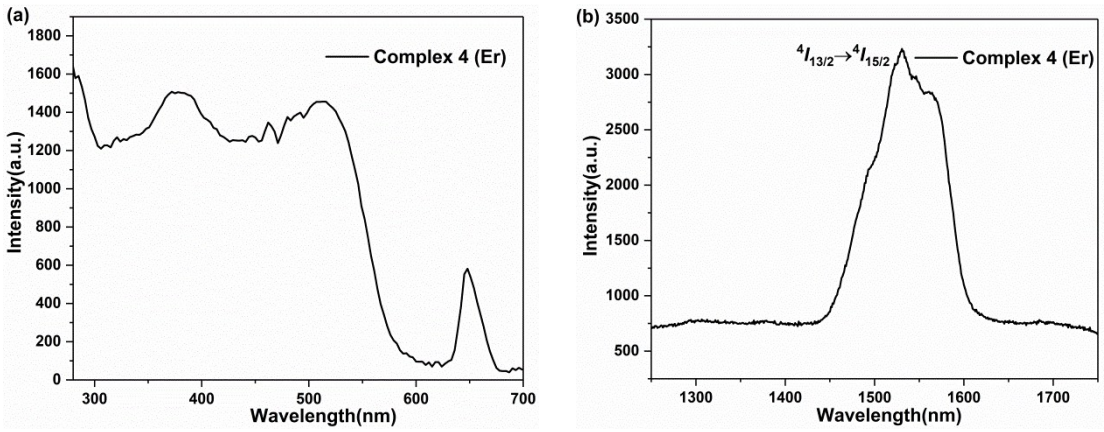

Fig. S5 (a) Excitation spectrum (λem = 1528 nm) and (b) emission spectrum of complex **4** (λex = 375 nm) in the solid state.

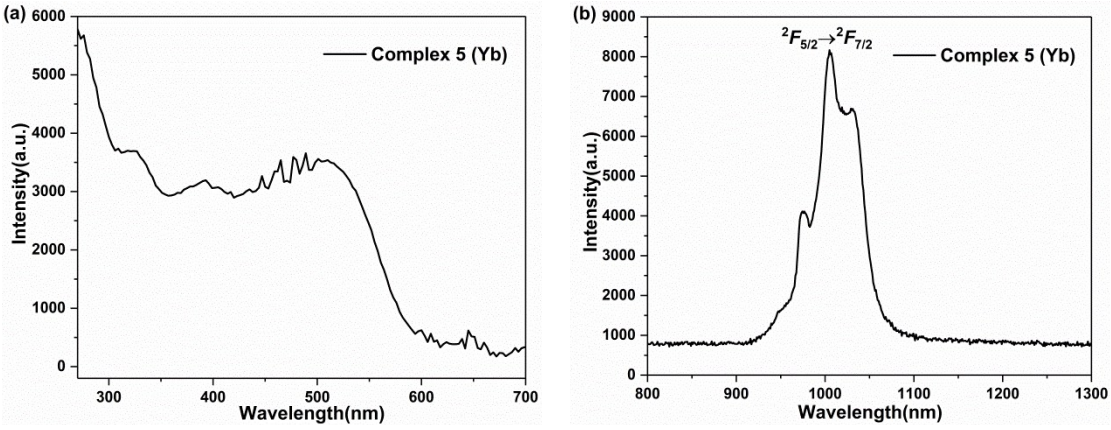

Fig. S6 (a) Excitation spectrum (λem = 975 nm) and (b) emission spectrum of complex **5** (λex = 510 nm) in the solid state.

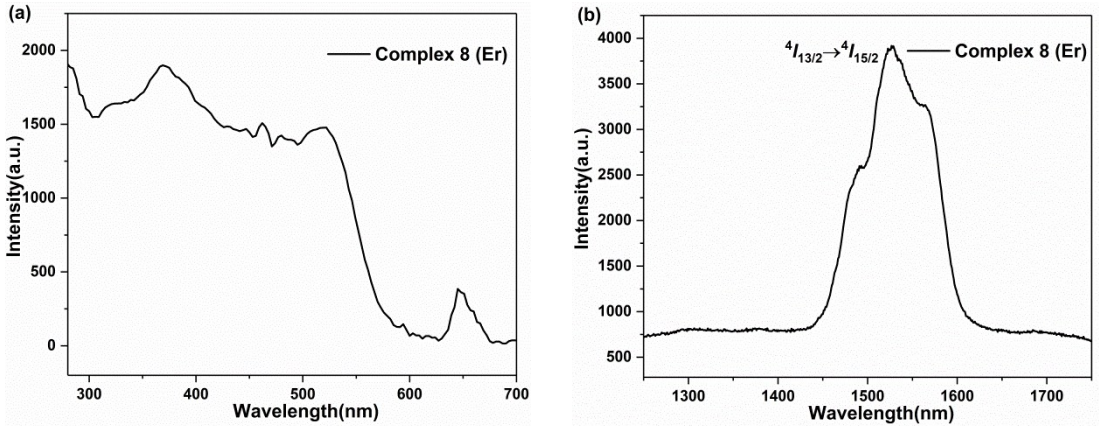

Fig. S7 (a) Excitation spectrum (λem = 1528 nm) and (b) emission spectrum of complex **8** (λex = 370 nm) in the solid state.

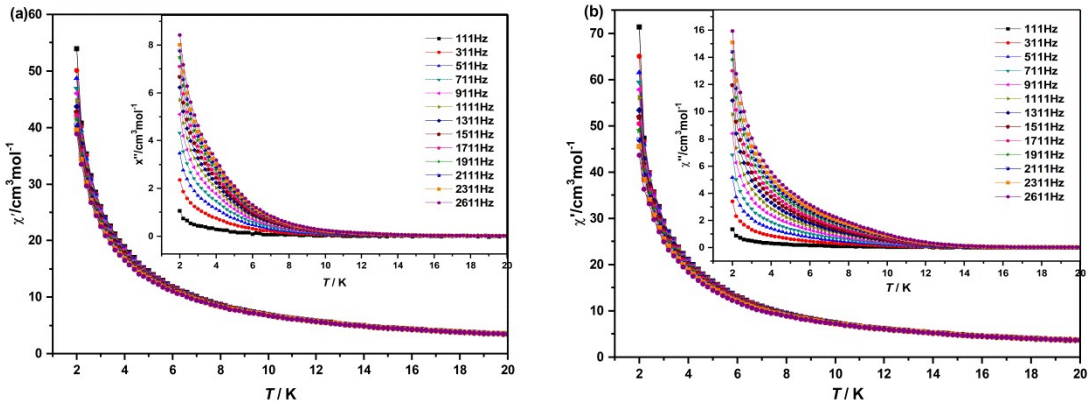

Fig. S8 Temperature dependence of χ' and χ'' for **2** (a) and **7**(b) in a zero static field and an oscillating field of 3 Oe (the solid lines connecting the data points are guides for the eye).

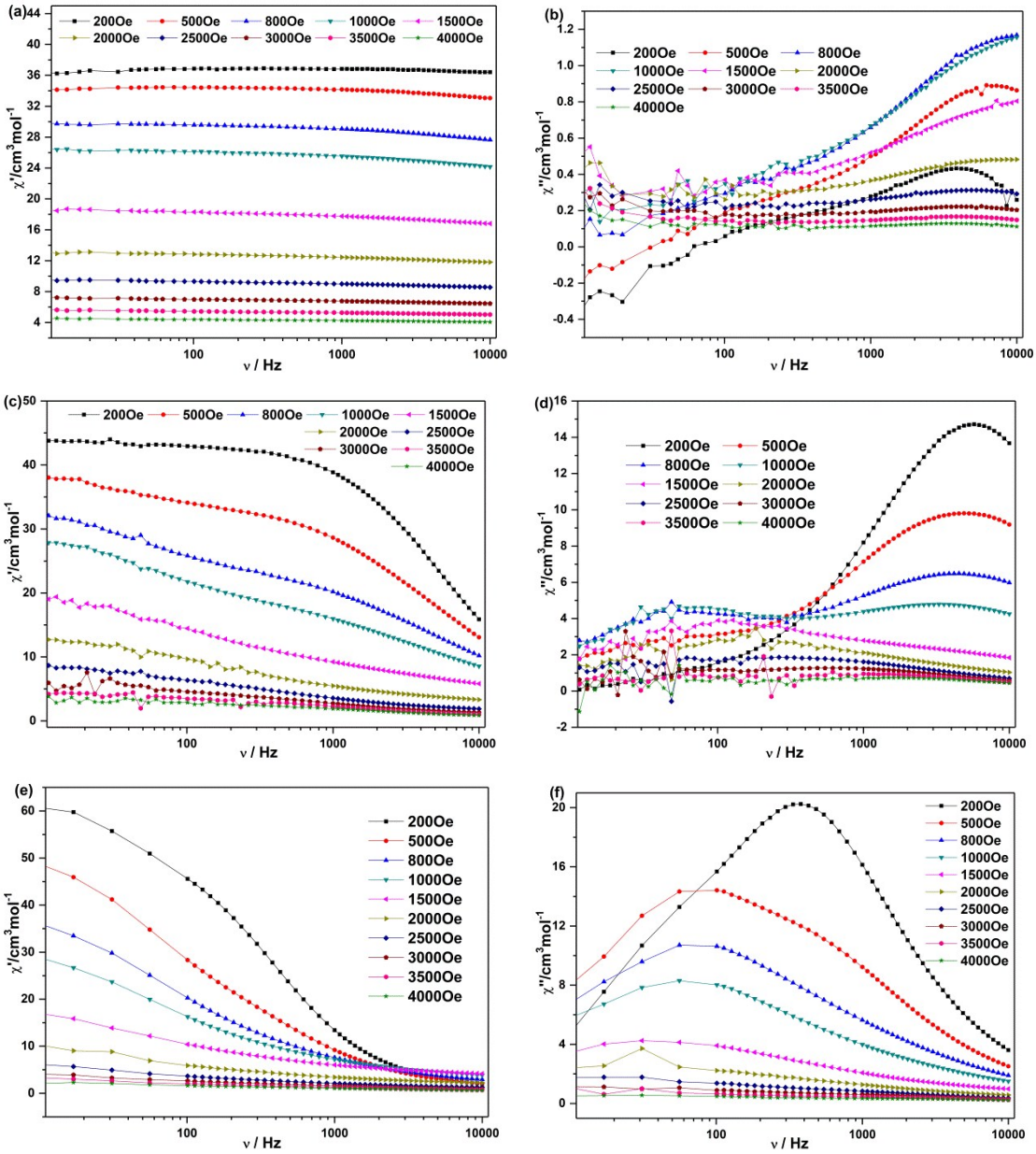

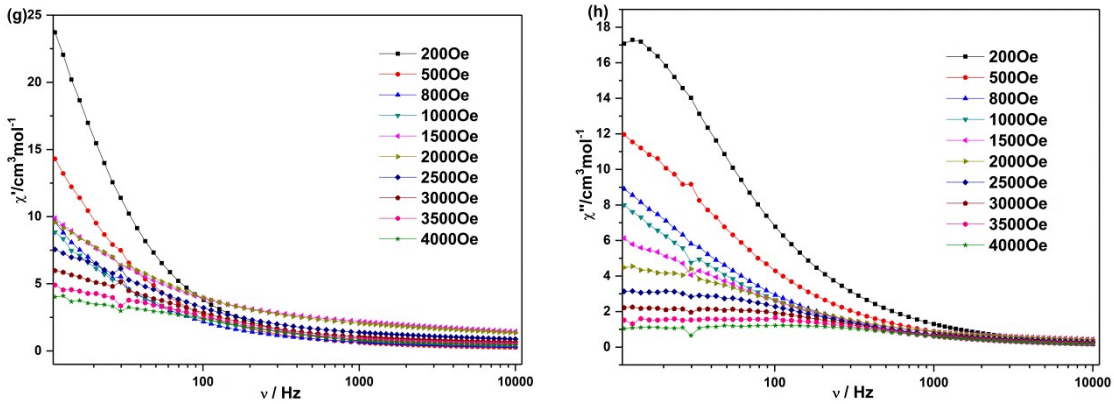

Fig. S9 Frequency dependency of the ac susceptibility was measured on **2** (a,b), **7**(c,d), **9**(e,f) and **10**(g,h) under the applied field from 200 to 4000 Oe at 2.0 K (the solid lines connecting the data points are guides for the eye).

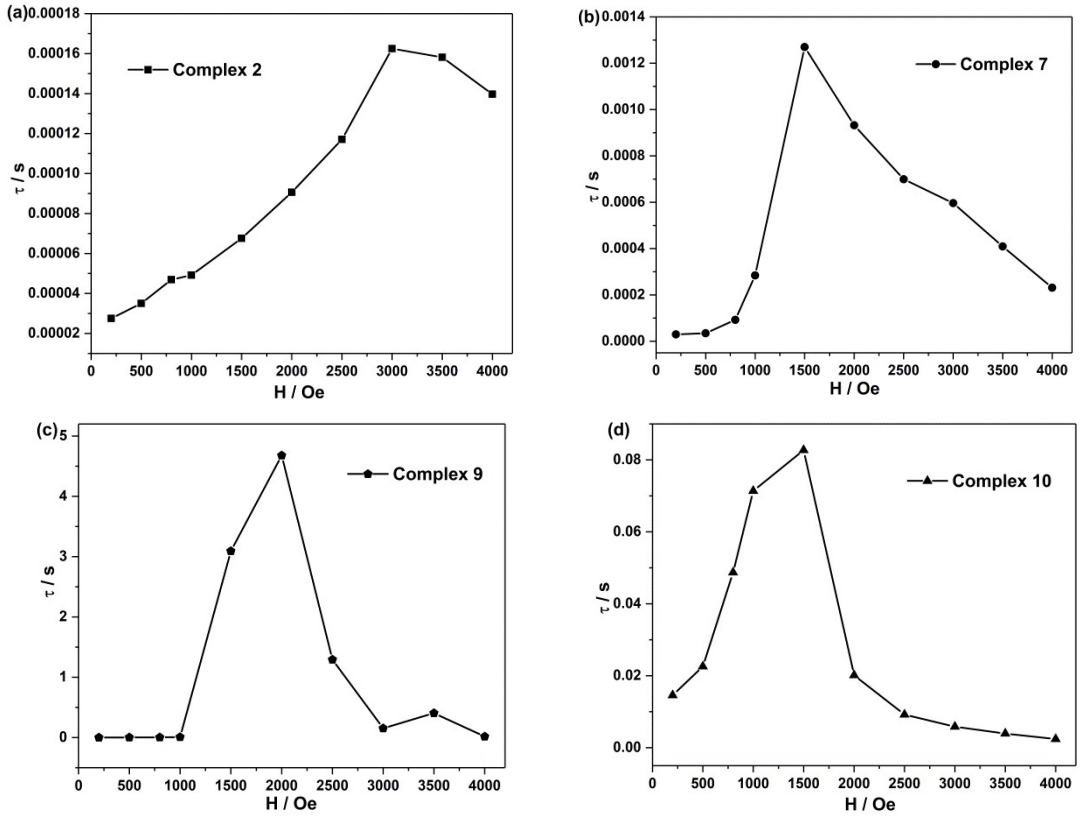

Fig. S10 Field dependence of the magnetic relaxation time (τ), at 2 K for **2** (a), **7**(b), **9**(c) and **10**(d).

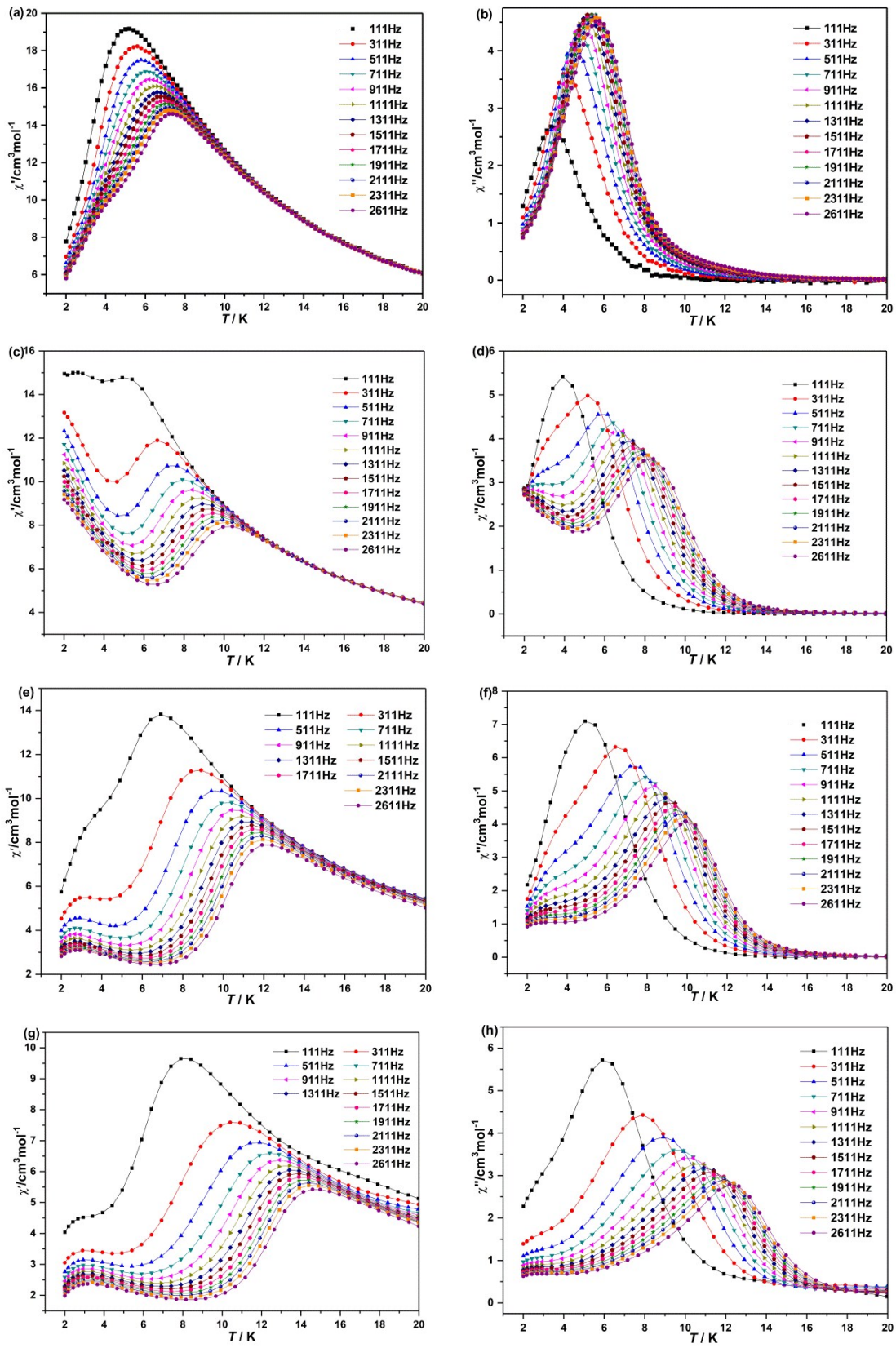

Fig. S11 Temperature dependence of χ' and χ'' for **2** (H_{dc} = 3000 Oe, a and b), **7** (H_{dc} = 1500 Oe, c and d), **9** (H_{dc} = 2000 Oe, e and f) and **10** (H_{dc} = 1500 Oe, g and h) in an oscillating field of 3 Oe. (the solid lines connecting the data points are guides for the eye).

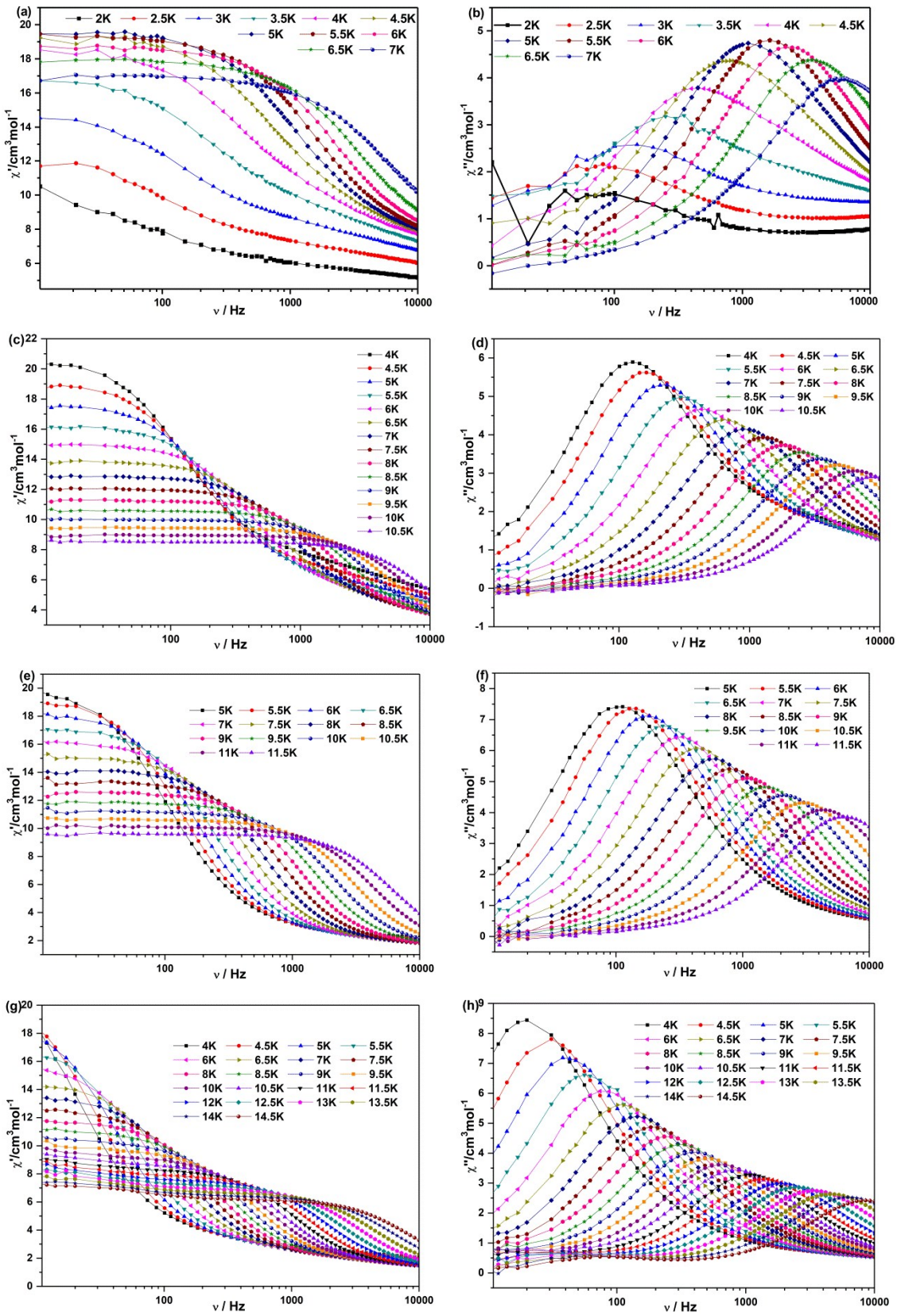

Fig. S12 Frequency dependence of χ' and χ'' for **2** (H_{dc} = 3000 Oe, a and b), **7** (H_{dc} = 1500 Oe, c and d), **9** (H_{dc} = 2000 Oe, e and f) and **10** (H_{dc} = 1500 Oe, g and h) in an oscillating field of 3 Oe. (the solid lines connecting the data points are guides for the eye).

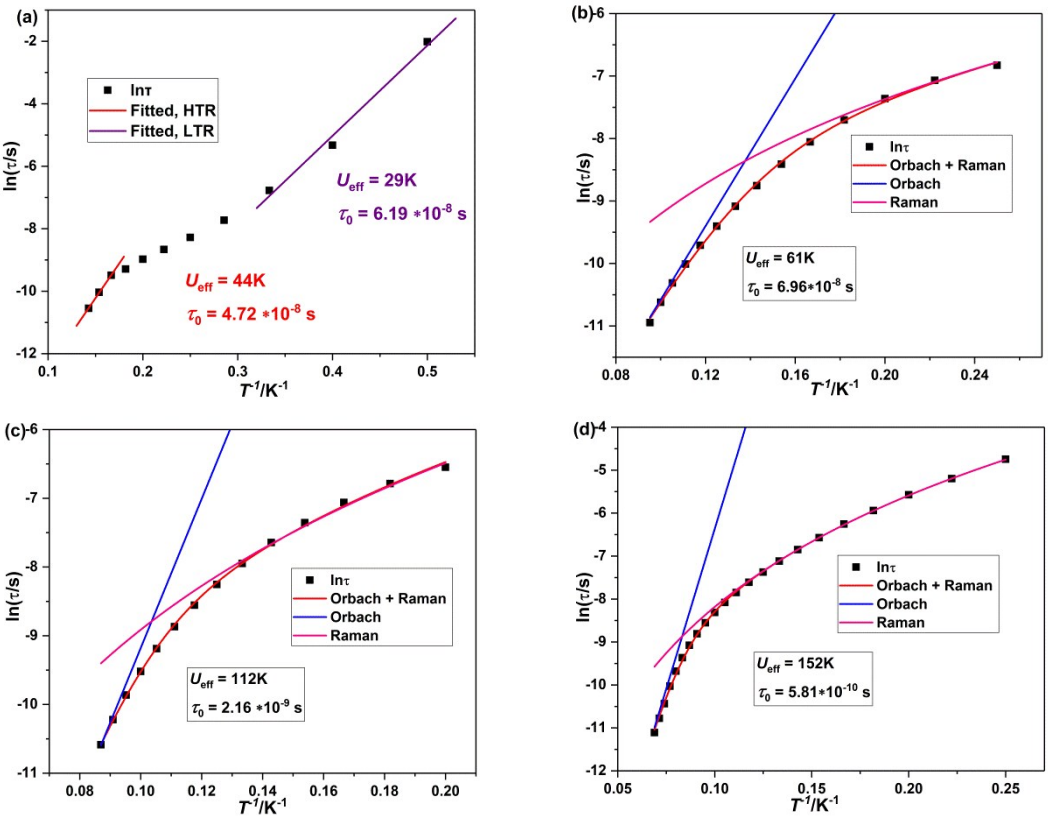

Fig. S13 The *ln(τ)* versus *1/T* plots of **2**(a, H_{dc} = 3000 Oe), **7**(b, H_{dc} = 1500 Oe), 9(c, H_{dc} = 2000 Oe) and 10(d) (H_{dc} = 1500 Oe); the red lines correspond to the best fit.

Table S1 Crystal data and structure refinement for complexes **1**–**5**

Complex	**1**	**2**	**3**	**4**	**5**
Formula	$C_{58}H_{50}N_8O_{10}Tb_2$	$C_{58}H_{50}N_8O_{10}Dy_2$	$C_{58}H_{50}N_8O_{10}Ho_2$	$C_{58}H_{50}N_8O_{10}Er_2$	$C_{58}H_{50}N_8O_{10}Yb_2$
Mr(g.mol^{-1})	1336.9	1344.06	1348.92	1353.58	1365.14
Temperature(K)	113(2)	113(2)	113(2)	113(2)	113(2)
Wavelength(Å)	0.71073	0.71073	0.71073	0.71073	0.71073
Crystal system	Orthorhombic	Orthorhombic	Orthorhombic	Orthorhombic	Orthorhombic
Space group	*P*bcn	*P*bcn	*P*bcn	*P*bcn	*P*bcn
a(Å)	22.133(4)	22.136(4)	22.114(4)	22.064(4)	22.018(4)
b(Å)	9.924(2)	9.903(2)	9.879(2)	9.869(2)	9.815(2)
c(Å)	24.477(5)	24.489(5)	24.526(5)	24.538(5)	24.552(5)
α(deg)	90	90	90	90	90
β(deg)	90	90	90	90	90
γ(deg)	90	90	90	90	90
Volume(Å3)	5376.3(19)	5368.3(19)	5357.9(19)	5343.4(19)	5306.1(18)
Z	4	4	4	4	4
Calculated density(Mg m^{-3})	1.652	1.663	1.672	1.683	1.709
Abs coeff(mm^{-1})	2.677	2.83	3.000	3.187	3.572
F(000)	2656	2664	2672	2680	2696
Crystal size(mm^3)	0.100x0.080	0.200x0.180	0.200x0.180	0.200x0.180	0.100x0.060

	x0.080	x0.120	x0.120	x0.120	x0.060
θ range(°)	2.880-25.018	2.801-25.018	1.842-25.019	1.660-25.017	1.659-27.898
Limiting indices	-26<=h<=26	-26<=h<=26	-26<=h<=26	-26<=h<=26	-28<=h<=28
	-11<=k<=11	-11<=k<=11	-11<=k<=11	-11<=k<=11	-12<=k<=12
	-29<=l<=29	-27<=l<=29	-25<=l<=29	-29<=l<=29	-32<=l<=26
Reflections collected	49077	40835	40550	48605	48474
Independent reflection	4719[R(int) =0.0843]	4717[R(int) =0.0738]	4721[R(int) =0.0794]	4681[R(int) =0.0923]	6301[R(int) =0.1118]
Completeness	99.50%	99.60%	99.90%	99.20%	99.90%
Max.and min. transmission	1 and 0.8188	1 and 0.8057	1 and 0.8318	1 and 0.8696	1 and 0.7919
Data/restraints /parameters	4719/12/355	4717/0/354	4721/12/354	4681/0/355	6301/24/355
GoF on F2	1.047	1.066	1.118	1.090	1.301
Final R indices[I>2σ(I)]	R_1^a = 0.0359, wR_2^b = 0.0851	R_1^a = 0.0358, wR_2^b = 0.0903	R_1^a = 0.0338, wR_2^b = 0.0677	R_1^a = 0.0412, wR_2^b = 0.0897	R_1^a = 0.0833, wR_2^b = 0.1397
R indices (all data)	R_1 = 0.0489, wR_2 = 0.0908	R_1 = 0.0465, wR_2 = 0.0966	R_1 = 0.0506, wR_2 = 0.0745	R_1 = 0.0610, wR_2 = 0.0979	R_1 = 0.1002, wR_2 = 0.1455
Largest diff.peak and hole(eÅ^{-3})	1.886 and -0.875	1.525 and -0.921	1.90 and -0.82	1.859 and -0.909	1.97 and -1.68

$^aR_1 = \sum(||F_o|-|F_c||)/\sum|F_o|$. $^bwR_2 = [\sum w(|F_o|^2-|F_c|^2)^2/\sum w(F_o^2)^2]^{1/2}$

Table S2 Crystal data and structure refinement for complexes **6–10**

Complex	**6**	**7**	**8**	**9**	**10**
Formula	$C_{58}H_{50}N_8O_{10}Lu_2$	$C_{40}H_{46}N_8O_{10}Dy_2$	$C_{40}H_{46}N_8O_{10}Er_2$	$C_{46}H_{38}Cl_4F_6N_8O_{10}S_2Dy_2$	$C_{40}H_{44}F_6N_8O_{12}Dy_2$
Mr(g.mol^{-1})	1369.00	1123.85	1133.37	1507.76	1267.83
Temperature(K)	113(2)	113(2)	113(2)	113(2)	113(2)
Wavelength(Å)	0.71073	0.71073	0.71073	0.71073	0.71073
Crystal system	Orthorhombic	Triclinic	Triclinic	Triclinic	Triclinic
Space group	*P*bcn	*P*$\bar{1}$	*P*$\bar{1}$	*P*$\bar{1}$	*P*$\bar{1}$
a(Å)	21.973(4)	9.4103(19)	9.4070(19)	10.583(2)	9.2010(18)
b(Å)	9.826(2)	11.313(2)	11.300(2)	11.808(2)	10.889(2)
c(Å)	24.585(5)	11.787(2)	11.706(2)	12.599(3)	12.038(2)
α(deg)	90	85.53(3)	85.25(3)	113.07(3)	73.38(3)
β(deg）	90	68.11(3)	68.20(3)	104.13(3)	85.05(3)
γ(deg)	90	67.45(3)	67.24(3)	102.28(3)	86.60(3)
Volume(Å^3)	5308.5(18)	1072.2(5)	1062.7(5)	1318.1(6)	1150.6(4)
Z	4	1	1	1	1
Calculated density(Mg m^{-3})	1.713	1.740	1.771	1.899	1.83
Abs coeff(mm^{-1})	3.766	3.523	3.987	3.180	3.315
F(000)	2704	554	558	*736*	622

Crystal size(mm^3)	0.200 x 0.180 x 0.120	0.200x0.180x0.120	0.200x0.180x0.120	0.200x0.180x0.120	0.200x0.180x0.120
θ range(°)	1.854 - 25.017	1.867-27.931	2.532 - 27.843	1.998-25.020	1.770-25.020
Limiting indices	-26<=h<=25 -11<=k<=11 -28<=l<=29	-12<=h<=12 -14<=k<=14 -15<=l<=15	-12<=h<=11 -14<=k<=14 -15<=l<=15	-12<=h<=12 -14<=k<=14 -14<=l<=14	-10<=h<=10 -12<=k<=12 - 14<=l<=14
Reflections collected	32676	12976	12448	12858	11171
Independent reflection	4680 [R(int) = 0.0721]	5103[R(int) = 0.0362]	5000 [R(int) = 0.0412]	4626 [R(int) = 0.0391]	4051[R(int) = 0.0496]
Completeness	99.9 %	99.90%	99.3%	99.7%	99.90%
Max.and min. transmission	1 and 0.6301	1 and 0.8323	1 and 0.6767	1 and 0.8529	1 and 0.4974
Data/restraints/parameters	4680 / 0 / 354	5103 /0 / 275	5000 / 0 / 275	4626 / 0 / 355	4051 / 18 / 312
GoF on F2	1.051	1.072	1.002	1.088	1.098
Final R indices[I>2σ(I)]	R_1^a = 0.0548, wR_2^b = 0.1760	R_1^a = 0.0262, wR_2^b = 0.0597	$R1^a$ = 0.0257, wR_2^b = 0.0653	R_1^a = 0.0386, wR_2^b = 0.1105	$R1^a$ = 0.0298, wR_2^b = 0.0745
R indices(all data)	R_1 = 0.0630, wR_2 = 0.1889	R_1 = 0.0299, wR_2 = 0.0613	R_1 = 0.0277, wR_2 = 0.0709	R_1 = 0.0440, wR_2 = 0.1387	R_1 = 0.0345, wR_2 = 0.0875
Largest diff.peak and hole($eÅ^{-3}$)	1.427 and -1.549	1.143 and -1.584	0.972 and -1.659	1.499 and -1.734	1.326 and -1.024

$^aR_1 = \sum(||F_o|-|F_c||)/\sum|F_o|$. $^bwR_2 = [\sum w(|F_o|^2-|F_c|^2)^2/\sum w(F_o^2)^2]^{1/2}$

Table S3 The important bond lengths (Å) and angles (°) for **1-10**

Complexes	The range of Ln–O bond lengths / Å	Average Ln–O bond lengths	The distance of Ln···Ln / Å	The Ln–O–Ln bond angles / °
1	2.219(3) - 2.406(3)	2.349(8)	3.9834(7)	112.80(12)
2	2.201(3) - 2.402(3)	2.339(5)	3.9733(7)	113.01(12)
3	2.207(3) - 2.383(3)	2.329(1)	3.9603(7)	113.30(12)
4	2.198(4) - 2.373(4)	2.317(2)	3.9487(7)	113.38(15)
5	2.175(5) - 2.358(6)	2.295(7)	3.9244(9)	114.2(2)
6	2.176(6) - 2.351(6)	2.294(3)	3.9139(9)	114.2(2)
7	2.202(2) - 2.433(2)	2.343(9)	3.9526(11)	112.30(8)
8	2.196(2) - 2.395(3)	2.313(9)	3.9228(11)	112.75(9)
9	2.196(5) - 2.414(5)	2.351(3)	3.992(2)	114.46(17)
10	2.173(3) - 2.458(3)	2.338(2)	3.9108(10)	111.70(12)

Table S4 The selected bond lengths (Å) and angles (°) for **2**

Dy(1)-O(2)	2.201(3)	Dy(1)-O(3)	2.326(3)
Dy(1)-O(4)	2.355(3)	Dy(1)-O(1)#1	2.363(3)
Dy(1)-O(5)	2.388(3)	Dy(1)-O(1)	2.402(3)
Dy(1)-N(4)	2.419(4)	Dy(1)-N(1)#1	2.575(4)
Dy(1)-Dy(1)#1	3.9733(7)		

Dy(1)#1-O(1)-Dy(1)	113.01(12)		
O(2)-Dy(1)-O(3)	76.23(12)	O(2)-Dy(1)-O(4)	131.42(11)
O(3)-Dy(1)-O(4)	71.10(11)	O(2)-Dy(1)-O(1)#1	146.54(11)
O(3)-Dy(1)-O(1)#1	112.04(11)	O(4)-Dy(1)-O(1)#1	80.27(10)
O(2)-Dy(1)-O(5)	75.77(12)	O(3)-Dy(1)-O(5)	142.35(11)
O(4)-Dy(1)-O(5)	146.17(10)	O(1)#1-Dy(1)-O(5)	80.17(11)
O(2)-Dy(1)-O(1)	126.28(11)	O(3)-Dy(1)-O(1)	143.15(11)
O(4)-Dy(1)-O(1)	72.57(10)	O(1)#1-Dy(1)-O(1)	66.99(12)
O(5)-Dy(1)-O(1)	74.45(11)	O(2)-Dy(1)-N(4)	74.01(12)
O(3)-Dy(1)-N(4)	101.50(11)	O(4)-Dy(1)-N(4)	78.41(12)
O(1)#1-Dy(1)-N(4)	131.30(11)	O(5)-Dy(1)-N(4)	94.41(12)
O(1)-Dy(1)-N(4)	64.98(11)	O(2)-Dy(1)-N(1)#1	86.75(12)
O(3)-Dy(1)-N(1)#1	78.51(12)	O(4)-Dy(1)-N(1)#1	119.61(12)
O(1)#1-Dy(1)-N(1)#1	64.66(11)	O(5)-Dy(1)-N(1)#1	75.27(12)
O(1)-Dy(1)-N(1)#1	126.11(11)	N(4)-Dy(1)-N(1)#1	160.01(12)
O(2)-Dy(1)-Dy(1)#1	148.63(9)	O(3)-Dy(1)-Dy(1)#1	134.98(8)
O(4)-Dy(1)-Dy(1)#1	73.65(7)	O(1)#1-Dy(1)-Dy(1)#1	33.80(7)
O(5)-Dy(1)-Dy(1)#1	74.72(8)	O(1)-Dy(1)-Dy(1)#1	33.18(7)
N(4)-Dy(1)-Dy(1)#1	97.86(8)	N(1)#1-Dy(1)-Dy(1)#1	95.84(8)

Symmetry transformations used to generate equivalent atoms: #1 -x+2,-y+1,-z+1

Table S5 The selected bond lengths (Å) and angles (°) for **7**

Dy(1)-O(2)#1	2.202(2)	Dy(1)-O(4)	2.321(2)
Dy(1)-O(3)	2.347(2)	Dy(1)-O(1)	2.368(2)
Dy(1)-O(1)#1	2.391(2)	Dy(1)-O(5)	2.433(2)
Dy(1)-N(4)#1	2.459(3)	Dy(1)-N(1)	2.548(2)
Dy(1)-Dy(1)#1	3.9526(11)		
Dy(1)-O(1)-Dy(1)#1	112.30(8)		
O(2)#1-Dy(1)-O(4)	75.74(9)	O(2)#1-Dy(1)-O(3)	133.02(8)
O(4)-Dy(1)-O(3)	71.71(8)	O(2)#1-Dy(1)-O(1)	144.05(7)
O(4)-Dy(1)-O(1)	118.68(8)	O(3)-Dy(1)-O(1)	82.25(7)
O(2)#1-Dy(1)-O(1)#1	122.74(8)	O(4)-Dy(1)-O(1)#1	142.18(8)
O(3)-Dy(1)-O(1)#1	72.59(7)	O(1)-Dy(1)-O(1)#1	67.70(8)
O(2)#1-Dy(1)-O(5)	74.98(8)	O(4)-Dy(1)-O(5)	140.66(8)
O(3)-Dy(1)-O(5)	146.92(7)	O(1)-Dy(1)-O(5)	74.88(8)
O(1)#1-Dy(1)-O(5)	76.72(7)	O(2)#1-Dy(1)-N(4)#1	73.51(8)
O(4)-Dy(1)-N(4)#1	96.21(8)	O(3)-Dy(1)-N(4)#1	77.33(8)
O(1)-Dy(1)-N(4)#1	131.09(7)	O(1)#1-Dy(1)-N(4)#1	63.89(8)
O(5)-Dy(1)-N(4)#1	100.04(8)	O(2)#1-Dy(1)-N(1)	90.60(8)
O(4)-Dy(1)-N(1)	76.04(8)	O(3)-Dy(1)-N(1)	112.73(8)
O(1)-Dy(1)-N(1)	64.54(7)	O(1)#1-Dy(1)-N(1)	130.33(7)

O(5)-Dy(1)-N(1)	78.57(8)	N(4)#1-Dy(1)-N(1)	163.73(8)
O(2)#1-Dy(1)-Dy(1)#1	144.31(6)	O(4)-Dy(1)-Dy(1)#1	139.95(6)
O(3)-Dy(1)-Dy(1)#1	74.83(6)	O(1)-Dy(1)-Dy(1)#1	34.04(5)
O(1)#1-Dy(1)-Dy(1)#1	33.67(5)	O(5)-Dy(1)-Dy(1)#1	72.82(6)
N(4)#1-Dy(1)-Dy(1)#1	97.33(6)	N(1)-Dy(1)-Dy(1)#1	97.70(6)

Symmetry transformations used to generate equivalent atoms: #1 -x+2,-y,-z+1

Table S6 The selected bond lengths (Å) and angles (°) for **9**

Dy(1)-O(2)	2.196(5)	Dy(1)-O(1)#1	2.366(5)
Dy(1)-O(4)	2.372(5)	Dy(1)-O(3)	2.375(5)
Dy(1)-O(1)	2.382(4)	Dy(1)-O(5)	2.414(5)
Dy(1)-N(4)	2.455(6)	Dy(1)-N(1)#1	2.556(6)
Dy(1)-Dy(1)#1	3.992(2)		
Dy(1)#1-O(1)-Dy(1)	114.46(17)		
O(2)-Dy(1)-O(1)#1	141.94(17)	O(2)-Dy(1)-O(4)	132.31(18)
O(1)#1-Dy(1)-O(4)	83.69(17)	O(2)-Dy(1)-O(3)	73.33(19)
O(1)#1-Dy(1)-O(3)	118.55(17)	O(4)-Dy(1)-O(3)	70.48(17)
O(2)-Dy(1)-O(1)	128.07(18)	O(1)#1-Dy(1)-O(1)	65.54(18)
O(4)-Dy(1)-O(1)	74.31(17)	O(3)-Dy(1)-O(1)	143.53(17)
O(2)-Dy(1)-O(5)	75.74(18)	O(1)#1-Dy(1)-O(5)	74.65(17)
O(4)-Dy(1)-O(5)	148.34(17)	O(3)-Dy(1)-O(5)	140.50(17)
O(1)-Dy(1)-O(5)	75.78(17)	O(2)-Dy(1)-N(4)	74.09(18)
O(1)#1-Dy(1)-N(4)	129.45(16)	O(4)-Dy(1)-N(4)	85.16(18)
O(3)-Dy(1)-N(4)	103.40(19)	O(1)-Dy(1)-N(4)	63.96(16)
O(5)-Dy(1)-N(4)	90.97(18)	O(2)-Dy(1)-N(1)#1	87.10(18)
O(1)#1-Dy(1)-N(1)#1	64.59(17)	O(4)-Dy(1)-N(1)#1	111.52(18)
O(3)-Dy(1)-N(1)#1	74.69(19)	O(1)-Dy(1)-N(1)#1	128.55(17)
O(5)-Dy(1)-N(1)#1	79.83(18)	N(4)-Dy(1)-N(1)#1	160.7(2)
O(2)-Dy(1)-Dy(1)#1	146.56(14)	O(1)#1-Dy(1)-Dy(1)#1	32.89(11)
O(4)-Dy(1)-Dy(1)#1	76.91(12)	O(3)-Dy(1)-Dy(1)#1	139.73(13)
O(1)-Dy(1)-Dy(1)#1	32.65(11)	O(5)-Dy(1)-Dy(1)#1	72.34(12)
N(4)-Dy(1)-Dy(1)#1	96.59(13)	N(1)#1-Dy(1)-Dy(1)#1	96.75(14)

Symmetry transformations used to generate equivalent atoms: #1 -x+1,-y+1,-z+2

Table S7 The selected bond lengths (Å) and angles (°) for **10**

Dy(1)-O(1)#1	2.173(3)	Dy(1)-O(4)	2.313(4)
Dy(1)-O(2)	2.351(3)	Dy(1)-O(3)	2.357(3)
Dy(1)-O(2)#1	2.375(3)	Dy(1)-O(5)	2.458(3)
Dy(1)-N(1)#1	2.487(4)	Dy(1)-N(3)	2.557(4)
Dy(1)-Dy(1)#1	3.9108(10)		
Dy(1)-O(2)-Dy(1)#1	111.70(12)		

O(1)#1-Dy(1)-O(4)	115.01(14)	O(1)#1-Dy(1)-O(2)	149.06(12)
O(4)-Dy(1)-O(2)	90.82(12)	O(1)#1-Dy(1)-O(3)	82.39(13)
O(4)-Dy(1)-O(3)	72.33(13)	O(2)-Dy(1)-O(3)	90.23(11)
O(1)#1-Dy(1)-O(2)#1	134.14(12)	O(4)-Dy(1)-O(2)#1	71.46(12)
O(2)-Dy(1)-O(2)#1	68.30(12)	O(3)-Dy(1)-O(2)#1	137.17(12)
O(1)#1-Dy(1)-O(5)	81.58(13)	O(4)-Dy(1)-O(5)	140.64(12)
O(2)-Dy(1)-O(5)	88.92(11)	O(3)-Dy(1)-O(5)	147.02(12)
O(2)#1-Dy(1)-O(5)	71.97(12)	O(1)#1-Dy(1)-N(1)#1	73.96(14)
O(4)-Dy(1)-N(1)#1	74.47(13)	O(2)-Dy(1)-N(1)#1	132.39(12)
O(3)-Dy(1)-N(1)#1	125.32(13)	O(2)#1-Dy(1)-N(1)#1	64.09(12)
O(5)-Dy(1)-N(1)#1	76.91(13)	O(1)#1-Dy(1)-N(3)	84.86(13)
O(4)-Dy(1)-N(3)	137.04(12)	O(2)-Dy(1)-N(3)	64.27(12)
O(3)-Dy(1)-N(3)	73.35(13)	O(2)#1-Dy(1)-N(3)	122.61(12)
O(5)-Dy(1)-N(3)	76.65(12)	N(1)#1-Dy(1)-N(3)	148.15(13)
O(1)#1-Dy(1)-Dy(1)#1	159.79(10)	O(4)-Dy(1)-Dy(1)#1	79.37(9)
O(2)-Dy(1)-Dy(1)#1	34.35(8)	O(3)-Dy(1)-Dy(1)#1	116.60(9)
O(2)#1-Dy(1)-Dy(1)#1	33.96(7)	O(5)-Dy(1)-Dy(1)#1	78.50(8)
N(1)#1-Dy(1)-Dy(1)#1	98.04(10)	N(3)-Dy(1)-Dy(1)#1	93.80(9)

Symmetry transformations used to generate equivalent atoms: #1 -x,-y+1,-z

Table S8 The continuous symmetry measurement value calculated by SHAPE 2.0 for complexes **1-10**

Complex	D_{4d}SAPR	D_{2d}TDD	C_{2v}JBTPR	C_{2v}BTPR
1	2.668	**1.405**	3.342	2.157
2	2.643	**1.344**	3.321	2.142
3	2.598	**1.336**	3.251	2.094
4	2.593	**1.313**	3.202	2.069
5	2.631	**1.233**	3.150	2.030
6	2.515	**1.170**	3.038	1.926
7	**2.059**	2.407	3.577	2.377
8	**2.006**	2.320	3.428	2.270
9	3.215	2.618	3.604	**2.311**
10	2.228	2.284	2.045	**1.467**

Table S9 The datapoints used for the construction of *lnτ* versus *1/T* curves for complexes **9** and **10**.

Complexes **9** (H_{dc} = 0 Oe)		Complexes **10** (H_{dc} = 0 Oe)	
lnτ	*1/T*	*lnτ*	*1/T*
-8.25044	0.2	-5.3613	0.25
-8.35306	0.18182	-5.87036	0.2
-8.44253	0.16667	-6.13459	0.18182
-8.55049	0.15385	-6.39157	0.16667

-8.68331	0.14286	-6.63566	0.15385
-8.76812	0.13699	-6.86345	0.14286
-8.85868	0.13158	-7.07122	0.13333
-8.95991	0.12658	-7.28336	0.125
-9.05817	0.12195	-7.50203	0.11765
-9.16403	0.11765	-7.69708	0.11111
-9.28743	0.11364	-7.88759	0.10526
-9.41403	0.10989	-8.09285	0.1
-9.53638	0.10638	-8.30554	0.09524
-9.67853	0.10309	-8.5447	0.09091
-9.82758	0.1	-8.78945	0.08696
-9.98308	0.09709	-9.055	0.08333
-10.16732	0.09434	-9.33042	0.08
-10.34166	0.09174	-9.62742	0.07692
-10.53852	0.08929	-9.94506	0.07407
-10.74871	0.08696	-10.24038	0.07143
		-10.55663	0.06897
		-10.86225	0.06667

Complexes **2** (H_{dc} = 3000 Oe)		Complexes **7** (H_{dc} = 1500 Oe)		Complexes **9** (H_{dc} = 2000 Oe)		Complexes **10** (H_{dc} = 1500 Oe)	
lnτ	*1/T*	*lnτ*	*1/T*	*lnτ*	*1/T*	*lnτ*	*1/T*
-2.01471	0.5	-6.82892	0.25	-6.54848	0.2	-4.7447	0.25
-5.32629	0.4	-7.06936	0.22222	-6.78708	0.18182	-5.19744	0.22222
-6.77578	0.33333	-7.36164	0.2	-7.06108	0.16667	-5.57268	0.2
-7.72885	0.28571	-7.70301	0.18182	-7.35519	0.15385	-5.94049	0.18182
-8.27913	0.25	-8.05425	0.16667	-7.64419	0.14286	-6.25531	0.16667
-8.66632	0.22222	-8.4114	0.15385	-7.94903	0.13333	-6.5716	0.15385
-8.97707	0.2	-8.7553	0.14286	-8.25475	0.125	-6.85172	0.14286
-9.28991	0.18182	-9.08482	0.13333	-8.55624	0.11765	-7.11727	0.13333
-9.49188	0.16667	-9.40335	0.125	-8.86882	0.11111	-7.37388	0.125
-10.03417	0.15385	-9.70962	0.11765	-9.18863	0.10526	-7.61239	0.11765
-10.54811	0.14286	-10.01044	0.11111	-9.51982	0.1	-7.84974	0.11111
		-10.31262	0.10526	-9.86402	0.09524	-8.08097	0.10526
		-10.62123	0.1	-10.22097	0.09091	-8.3125	0.1
		-10.94756	0.09524	-10.5863	0.08696	-8.55454	0.09524
						-8.80868	0.09091
						-9.0773	0.08696
						-9.36573	0.08333
						-9.67829	0.08
						-10.0306	0.07692
						-10.43863	0.07407
						-10.77683	0.07143

						-11.11099	0.06897

1. (a) H. Tian, L. Zhao, Y. N. Guo, Y. Guo, J. Tang and Z. Liu, *Chem. Commun.*, 2012, **48**, 708; (b) H. Tian, S. S. Bao and L. M. Zheng, *Chem. Commun.*,2016, **52**, 2314; (c) H. Tian, Lang. Zhao and J. Tang, *Cryst. Growth Des.*, 2018, 18, 1173.